HHS Public Access

Author manuscript

Science. Author manuscript; available in PMC 2015 May 22.

Published in final edited form as:

Science. 2015 March 27; 347(6229): 1485–1489. doi:10.1126/science.aaa5267.

Spring-loaded unraveling of a single SNARE complex by NSF in one round of ATP turnover

Je-Kyung Ryu[1,2,*], **Duyoung Min**[1,2,*], **Sang-Hyun Rah**[1,2,*], **Soo Jin Kim**[3], **Yongsoo Park**[4], **Haesoo Kim**[3], **Changbong Hyeon**[5], **Ho Min Kim**[3], **Reinhard Jahn**[4,†], and **Tae-Young Yoon**[1,2,†]

[1]National Creative Research Initiative Center for Single-Molecule Systems Biology, Korea Advanced Institute of Science and Technology (KAIST), Daejeon 305-701, South Korea.

[2]Department of Physics, KAIST, Daejeon 305-701, South Korea.

[3]Graduate School of Medical Science and Engineering, KAIST, Daejeon 305-701, South Korea.

[4]Department of Neurobiology, Max-Planck-Institute for Biophysical Chemistry, 37077 Göttingen, Germany.

[5]Korea Institute for Advanced Study, Seoul 130-722, South Korea.

Abstract

During intracellular membrane trafficking, *N*-ethylmaleimide-sensitive factor (NSF) and alpha-soluble NSF attachment protein (α-SNAP) disassemble the soluble NSF attachment protein receptor (SNARE) complex for recycling of the SNARE proteins. The molecular mechanism by which NSF disassembles the SNARE complex is largely unknown. Using single-molecule fluorescence spectroscopy and magnetic tweezers, we found that NSF disassembled a single SNARE complex in only one round of adenosine triphosphate (ATP) turnover. Upon ATP cleavage, the NSF hexamer developed internal tension with dissociation of phosphate ions. After latent time measuring tens of seconds, NSF released the built-up tension in a burst within 20 milliseconds, resulting in disassembly followed by immediate release of the SNARE proteins. Thus, NSF appears to use a “spring-loaded” mechanism to couple ATP hydrolysis and unfolding of substrate proteins.

Soluble *N*-ethylmaleimide-sensitive factor (NSF) attachment protein receptor (SNARE) proteins are the essential molecular machinery for intracellular membrane fusion in eukaryotic cells (1). Synaptic exocytosis is among the best studied, in which synaptic

[†]Corresponding author. rjahn@gwdg.de (R.J.); tyyoon@kaist.ac.kr (T.-Y.Y.).
[*]These authors contributed equally to this work.

SUPPLEMENTARY MATERIALS

www.sciencemag.org/content/347/6229/1485/suppl/DC1

Materials and Methods
Supplementary Text
Figs. S1 to S17
Table S1
References (32–69)

vesicle–associated VAMP2 engages with syntaxin-1A and SNAP-25 on the presynaptic membrane to form the neuronal SNARE complex (2, 3). Although the formed SNARE complex is very stable after synaptic vesicle fusion (4–6), the complex must be disassembled for reuse of the SNARE proteins, requiring a specialized molecular machinery, consisting of NSF and alpha-soluble NSF attachment protein (α-SNAP) (7–12).

NSF belongs to the type II adenosine triphosphatase associated with various cellular activities (AAA+) family, which assembles into a homohexamer (13–15). Despite the fundamental role of NSF in synaptic transmission (7, 9, 16), surprisingly little is known about how its adenosine triphosphate (ATP) hydrolysis cycle is coupled to disassembly of the SNARE complex. The NSF hexamer may disassemble a SNARE complex by unwinding it in a processive manner, similar to translocation of AAA+ adenosine triphosphatases (ATPases) on DNA or peptide substrates (17, 18). Alternatively, NSF may exploit a critical conformational transition to evoke the disassembly of the SNARE complex largely in one step (19). It is not clear how many cycles of ATP hydrolysis are needed and how these cycles are organized to disassemble the extraordinarily stable SNARE complex.

To gain insight into these questions, we first formed single SNARE complexes on surface-immobilized vesicles (20, 21), which were observed as single-molecule fluorescence spots when viewed with total internal reflection (TIR) microscopy (Fig. 1A and B, and fig. S1). Here the soluble part of VAMP2 was used and labeled with the Cy3 dye. We subsequently injected α-SNAP and then the NSF hexamers (2, 11, 12) along with ATP and Mg^{2+} ions (Fig. 1A, and C, and fig. S1A). After 5 min of reaction, we counted the number of fluorescence spots.

We observed that the fluorescence spots disappeared only when α-SNAP, NSF, ATP, and Mg^{2+} were added (Fig. 1, B and D). When any one component was missing or either nonhydrolyzable ATPγS or α-SNAP L294A mutant that abolished ATP hydrolysis in NSF (22) was used, no disappearance of Cy3-labeled spots was observed (Fig. 1D). Thus, the disappearance of Cy3 spots strictly depended on the presence of both α-SNAP and NSF and also on ATP hydrolysis by NSF, indicating that the disassembly of single SNARE complexes induced by NSF and α-SNAP was reconstituted on our single-molecule fluorescence microscope.

We next attempted to differentiate between NSF binding and ATP hydrolysis. This time, we introduced NSF with ATP and EDTA to induce ATP-dependent NSF binding but without hydrolysis of ATP molecules (Fig. 1E). Using labelled antibodies, we were able to confirm sequential binding of α-SNAP and NSF (Fig. 1, F and G, and fig. S2, A to C). After formation of the immobilized 20*S* complexes (NSF/ α-SNAP/SNARE complex), we performed washing and injected Mg^{2+} and ATP. We observed disassembly of single SNARE complexes, indicating that single NSF-binding was sufficient for the disassembly (Fig. 1H). Moreover, we observed the SNARE complex disassembly when we injected only Mg^{2+} ions (Fig. 1H). Because free ATP molecules were completely removed before Mg^{2+} injection, the disassembly was exclusively mediated by hydrolysis of the ATP molecules already bound to NSF. By imaging disassembly with high temporal resolution (fig. S2, F and G), we confirmed that the disassembly using only one-round ATP turnover was as fast

as that observed in the presence of excess NSF and ATP (Fig. 1I). Thus, binding of a single NSF hexamer and only one round of ATP hydrolysis in NSF was sufficient for disassembly of a single neuronal SNARE complex.

To explore how such a tight coupling between ATP hydrolysis and NSF activity can be achieved, we used single-molecule fluorescence resonance energy transfer (FRET) (23). We labeled either the N- or C-terminal end of the SNARE motif with the Cy3-Cy5 pair (Fig. 2A and fig. S3). We observed that α-SNAP induces destabilization of the C-terminal part of the SNARE complex, albeit to different extents for individual SNARE complexes (fig. S4) (11, 24). Next, we added NSF and followed the protocol, allowing only one round of ATP hydrolysis (Fig. 2B). Notably, when we measured FRET at the C-terminal end ($E_{C\text{-}term}$), the donor and acceptor fluorescence signals initially remained stationary and then disappeared all of a sudden (Fig. 2, C and D, and fig. S5). Such behaviour was found in more than 96% of the entire time-resolved traces even when the traces started from a high FRET state (Fig. 2E and fig. S6). Thus, after a quiescent waiting time, the SNARE complex was disassembled in one step, and the Cy3-labeled sVAMP2 was immediately released from the 20*S* complex after disassembly. We repeated the time-resolved measurements with the N-terminal FRET pair ($E_{N\text{-}term}$), and 95% of the real-time traces showed the one-step disassembly pattern (Fig. 2E and fig. S5). We also observed disassembly in the presence of free NSF and ATP. For both N- and C-terminal FRET pairs, the traces predominantly showed the one-step disassembly (Fig. 2E and fig. S5). Finally, we observed disassembly of the SNARE complexes in their native configuration, with both syntaxin-1A and full-length VAMP2 anchored to the same membrane (Fig. 2F and fig. S7). Once again, one-step disassembly comprised ~90% of the total traces obtained during both disassembly via one-round ATP hydrolysis and with free NSF and ATP (Fig. 2G and fig. S8). Thus, the NSF hexamer disassembled the entire SNARE complex in a single burst and released the disassembled, individual SNARE components immediately after disassembly.

Next, we wanted to gain more mechanistic insights into the disassembly reaction using single-molecule force spectroscopy (4, 25–27). While pulling a single SNARE complex with 3.9 pN force, we introduced α-SNAP followed by a mixture of NSF, ATP, and Mg^{2+} ions (Fig. 3, A to C, and figs. S9 to S13). Upon addition of α-SNAP and NSF, the extension was largely maintained at the same level, although the distribution became broader and the extension peak was slightly shifted to higher values (Fig. 3D). Notably, in about half of all experiments, the connection was lost abruptly with a characteristic latency of 71.4 s. (Fig. 3A, red arrow, and fig. S14). Such abrupt disappearance of the signal indicates that the tweezed SNARE complex was disassembled within our time resolution (16.7 ms) and the disassembled SNARE proteins were immediately released from the 20*S* complex, concordant with our single-molecule FRET data. In the other half of the traces, the extension value showed a sudden increase and stayed there for a few seconds before complete release (Fig. 3B). The extension burst corresponded to disassembly up to the N-terminal end of the SNARE motif and was completed within 21.8 ms (Fig. 3E, pink distributions, and fig. S15). Thus, we conclude that virtually in all the observed traces, the SNARE complex was disassembled by NSF in one step even when resolved at a time resolution of 16.7 ms. Finally, we observed rare events where the SNARE complex showed repetitive unzipping

and rezipping (Fig. 3C), giving a hint as to why it is important to instantly release the SNARE proteins after the disassembly. The repeated failures suggest either that some SNARE complexes are more difficult to unzip or that certain 20*S* complexes show a looser coupling between ATP hydrolysis in NSF and SNARE complex disassembly.

The question then arises how exactly the burst disassembly is coupled to the steps of the given, single ATP hydrolysis cycle. To answer this final question, we replicated our disassembly experiment with one difference: that free phosphate ions (Pis) or Pi analogs were added along with Mg^{2+} ions (Fig. 4A). Addition of free Pis up to 10 mM only minimally affected disassembly (Fig. 4B). However, a Pi analog, orthovanadate (VO_4^{3-}), significantly inhibited the disassembly at 1 μM concentration (Fig. 4C). Addition of a different Pi analog, 10 μM AlFx, also inhibited disassembly. In addition, 1 μM VO_4^{3-} impeded the disassembly of the SNARE complexes with full-length VAMP2 (Fig. 4, D and E).Given that the Pi analogs used here (but not Pi) selectively stabilize a transition state containing adenosine diphosphates (ADPs) (28, 29), we suggest that NSF is overall bound with ADP during the latent time before disassembly.

Our observations suggest two alternative models for the NSF function (fig. S16). First, the disassembly is precisely coupled to the release of Pis, which is also the force-generating step for the translocational motion of ClpXP and ϕ29 (17, 30). In this “power-stroke” model, release of Pis from the subunits of NSF can occur in a predetermined order (18, 30), which may be viewed as processive unwinding of the SNARE complex (Fig. 4F). The second model implies that ATP hydrolysis and Pi release need to be completed first to initiate disassembly. Because the SNARE complex resists disassembly, NSF is trapped in the conformation of the ATP-bound state while it is actually bound to ADP. Mechanical tension develops within the NSF hexamer and then is delivered to the SNARE complex. In this “spring-loaded” model, NSF tears the SNARE complex into individual SNARE proteins upon brief destabilization of the SNARE complex by thermal fluctuations (Fig. 4G).

These two models are distinguished by the type of nucleotides bound to NSF during the latent time before disassembly. In the power-stroke model, the NSF hexamer will remain in the ATP-bound state, whereas in the spring-loaded model, NSF will be essentially bound to ADP during the latent time (Fig. 4, F and G). Our experimental data, in particular those using Pi analogs, favor the spring-loaded model for the NSF function. With the spring-loaded model, NSF takes advantage of thermal fluctuations, eventually unraveling the target SNARE complex if a long latent time is given (fig. S17). We presume that the Pi analogs diminish the internal strain in the 20*S* complex and impede the disassembly process. We cannot rule out the possibility that the Pi analogs negatively affect the 20*S* particles in a way other than described here. Detailed conformational changes involved in disassembly remain unclear (31). Because the AAA domains are highly conserved, the spring-loaded mechanism elucidated here for NSF may be shared by many other AAA+ ATPases, which provides a way to tightly couple their ATP hydrolysis and unfolding of protein substrates.

Supplementary Material

Refer to Web version on PubMed Central for supplementary material.

ACKNOWLEDGMENTS

We thank J. Jo and B. Choi for help with preparing illustrations and S. E. Lee for help with single-molecule analysis. This work was supported by the National Creative Research Initiative Program (Center for Single-Molecule Systems Biology to T.-Y.Y.) and a grant (NRF-2012R1A1A1010456 to H.M.K.) through the National Research Foundation of Korea (NRF) funded by the Korean government. Funding was also generously provided by the National Institutes of Health (3P01GM072694-05S1 to R.J.).

REFERENCES AND NOTES

1. Söllner T, et al. Nature. 1993; 362:318–324. [PubMed: 8455717]
2. Hanson PI, Roth R, Morisaki H, Jahn R, Heuser JE. Cell. 1997; 90:523–535. [PubMed: 9267032]
3. Sutton RB, Fasshauer D, Jahn R, Brunger AT. Nature. 1998; 395:347–353. [PubMed: 9759724]
4. Min D, et al. Nat. Commun. 2013; 4:1705. [PubMed: 23591872]
5. Gao Y, et al. Science. 2012; 337:1340–1343. [PubMed: 22903523]
6. Li F, et al. Nat. Struct. Mol. Biol. 2007; 14:890–896. [PubMed: 17906638]
7. Wilson DW, et al. Nature. 1989; 339:355–359. [PubMed: 2657434]
8. Whiteheart SW, et al. Nature. 1993; 362:353–355. [PubMed: 8455721]
9. Söllner T, Bennett MK, Whiteheart SW, Scheller RH, Rothman JE. Cell. 1993; 75:409–418. [PubMed: 8221884]
10. Winter U, Chen X, Fasshauer D. J. Biol. Chem. 2009; 284:31817–31826. [PubMed: 19762473]
11. Chang LF, et al. Nat. Struct. Mol. Biol. 2012; 19:268–275. [PubMed: 22307055]
12. Moeller A, et al. J. Struct. Biol. 2012; 177:335–343. [PubMed: 22245547]
13. Lenzen CU, Steinmann D, Whiteheart SW, Weis WI. Cell. 1998; 94:525–536. [PubMed: 9727495]
14. Yu RC, Hanson PI, Jahn R, Brünger AT. Nat. Struct. Biol. 1998; 5:803–811. [PubMed: 9731775]
15. Nagiec EE, Bernstein A, Whiteheart SW. J. Biol. Chem. 1995; 270:29182–29188. [PubMed: 7493945]
16. Zhao C, Matveeva EA, Ren Q, Whiteheart SW. J. Biol. Chem. 2010; 285:761–772. [PubMed: 19887446]
17. Aubin-Tam ME, Olivares AO, Sauer RT, Baker TA, Lang MJ. Cell. 2011; 145:257–267. [PubMed: 21496645]
18. Sen M, et al. Cell. 2013; 155:636–646. [PubMed: 24243020]
19. Weber-Ban EU, Reid BG, Miranker AD, Horwich AL. Nature. 1999; 401:90–93. [PubMed: 10485712]
20. Pobbati AV, Stein A, Fasshauer D. Science. 2006; 313:673–676. [PubMed: 16888141]
21. Yoon TY, Okumus B, Zhang F, Shin YK, Ha T. Proc. Natl. Acad. Sci. U.S.A. 2006; 103:19731–19736. [PubMed: 17167056]
22. Barnard RJ, Morgan A, Burgoyne RD. J. Cell Biol. 1997; 139:875–883. [PubMed: 9362506]
23. Ha T, et al. Proc. Natl. Acad. Sci. U.S.A. 1996; 93:6264–6268. [PubMed: 8692803]
24. Park Y, et al. J. Biol. Chem. 2014; 289:16326–16335. [PubMed: 24778182]
25. Greenleaf WJ, Woodside MT, Block SM. Annu. Rev. Biophys. Biomol. Struct. 2007; 36:171–190. [PubMed: 17328679]
26. Moffitt JR, Chemla YR, Smith SB, Bustamante C. Annu. Rev. Biochem. 2008; 77:205–228. [PubMed: 18307407]
27. De Vlaminck I, Dekker C. Annu Rev Biophys. 2012; 41:453–472. [PubMed: 22443989]
28. Shimizu T, Johnson KA. J. Biol. Chem. 1983; 258:13833–13840. [PubMed: 6227617]
29. Davies DR, Hol WGJ. FEBS Lett. 2004; 577:315–321. [PubMed: 15556602]
30. Chemla YR, et al. Cell. 2005; 122:683–692. [PubMed: 16143101]
31. Zhao M, et al. Nature. 2015; 518:61–67. [PubMed: 25581794]

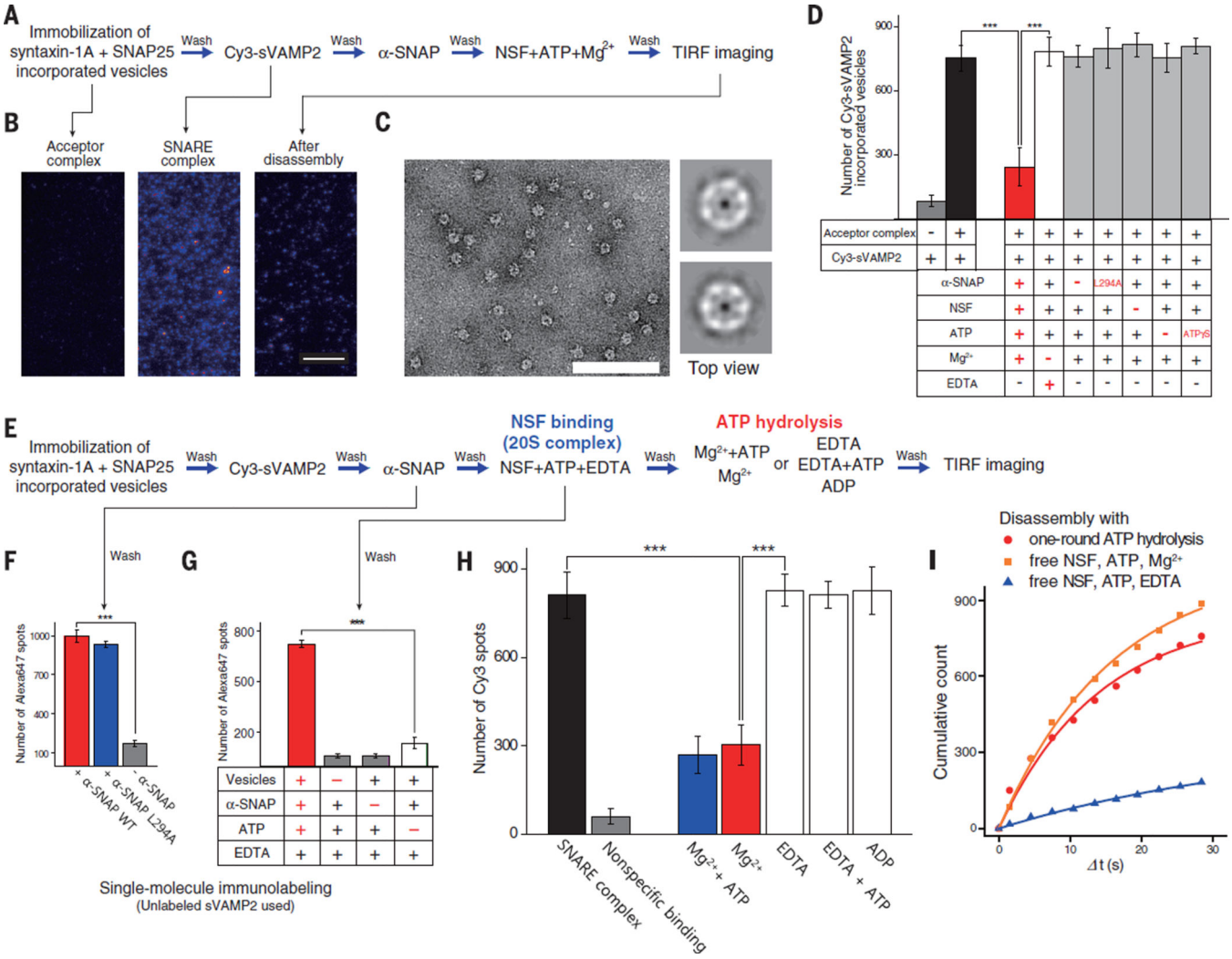

Fig. 1. Reconstitution of NSF-mediated SNARE complex disassembly on a single-molecule fluorescence microscope

(**A**) Procedure of the experiment. (**B**) Exemplary TIR microscopy images after immobilization of acceptor vesicles (left), after SNARE complex formation (middle), and after disassembly reaction (right). Scale bar, 10 μm. (**C**) NSF imaged using negative stain electron microscopy (left). Scale bar, 100 nm. Representative two-dimensional class averages (right). Top views are shown. (**D**) Number of surface vesicles containing Cy3-sVAMP2 measured with various components of the disassembly reaction. (Left) Nonspecific binding of sVAMP2 in the absence of acceptor vesicles (dark gray). Disassembly (loss of fluorescence) is observable only when all components required for disassembly are present (red bar). ***$P < 0.001$, assessed using the paired t test, and all the errors are SD ($n \geq 20$ TIR images) unless otherwise specified. (**E**) Procedure to allow for one-round ATP hydrolysis during the disassembly reaction. (**F** and **G**) Single-molecule immunolabeling assays for confirmation of α-SNAP-binding (F) and NSF-binding (G). Number of Alexa647 spots measured after incubation with the depicted components of the disassembly reaction. (**H**) Number of vesicles containing Cy3-sVAMP2 measured after SNARE complex formation (black), nonspecific binding of Cy3-sVAMP2 (gray), and after

the experimental protocol in (E) with Mg^{2+} and ATP (blue) or with Mg^{2+} (red). Other bars indicate control experiments where, instead of Mg^{2+}, either EDTA only, EDTA and ATP, or ADP (white) were injected during the ATP hydrolysis step. (**I**) Cumulative distributions of Δt for disassembly under conditions of one round of ATP hydrolysis and in the presence of excess NSF, ATP, and Mg^{2+}. Δt was measured from $t = 0$ to the event of stepwise fluorescence decrease (fig. S2, F and G). Fitting of the distributions using a single exponential function gives time constants of 15.8 ± 1.1 s and 14.1 ± 1.9 s for disassembly with one-round ATP hydrolysis and free NSF, ATP, and Mg^{2+}, respectively.

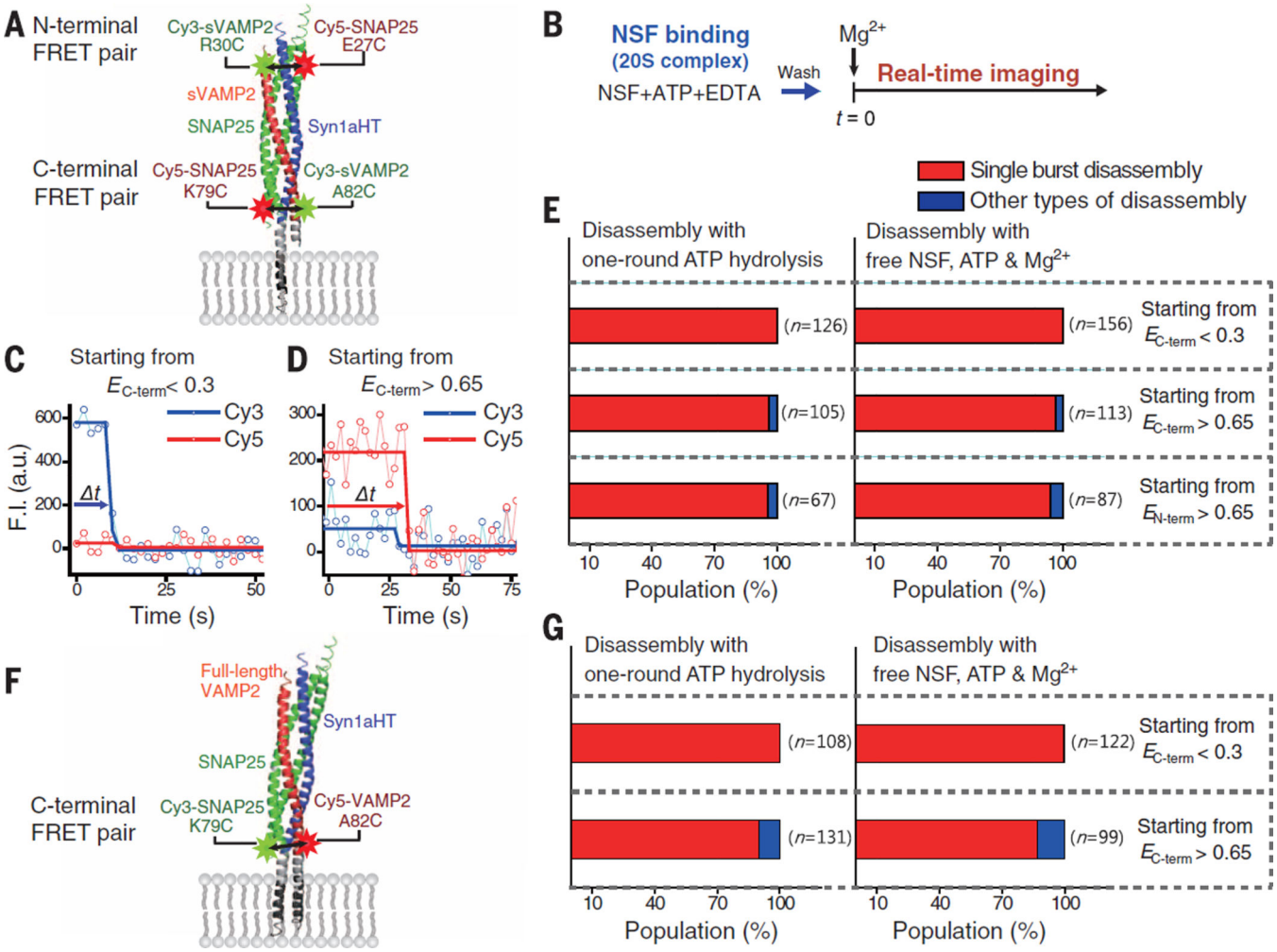

Fig. 2. Intermediates of NSF/α-SNAP disassembly of SNARE complex monitored by single-molecule FRET

(**A**) Labeling positions of Cy3 and Cy5 on either the N-terminal or the C-terminal end of the SNARE complex. According to the crystal structure (3), the expected distance between two dyes is less than 1.4 nm for both cases. (**B**) Experimental procedure. NSF, ATP, and EDTA were injected into the chamber containing α-SNAP-SNARE complexes. Movies were recorded starting at the same time as the injection of Mg^{2+}. (**C** and **D**) Representative disassembly traces of C-terminal FRET pairs starting from low FRET (<0.3) (C) and high FRET (>0.65) (D). (**E**) Relative abundance of disassembly events classified as single burst (red) and other types (blue). Disassembly was carried out under one-round ATP hydrolysis condition (left) or with excess NSF, ATP, and Mg^{2+} (right). (**F**) Labeling positions of Cy3 and Cy5 on the C-terminal end of the SNARE complex with full-length VAMP2. (**G**) Relative abundance of disassembly events classified as single burst (red) and other types (blue) using C-terminal FRET of SNARE complex with full-length VAMP2.

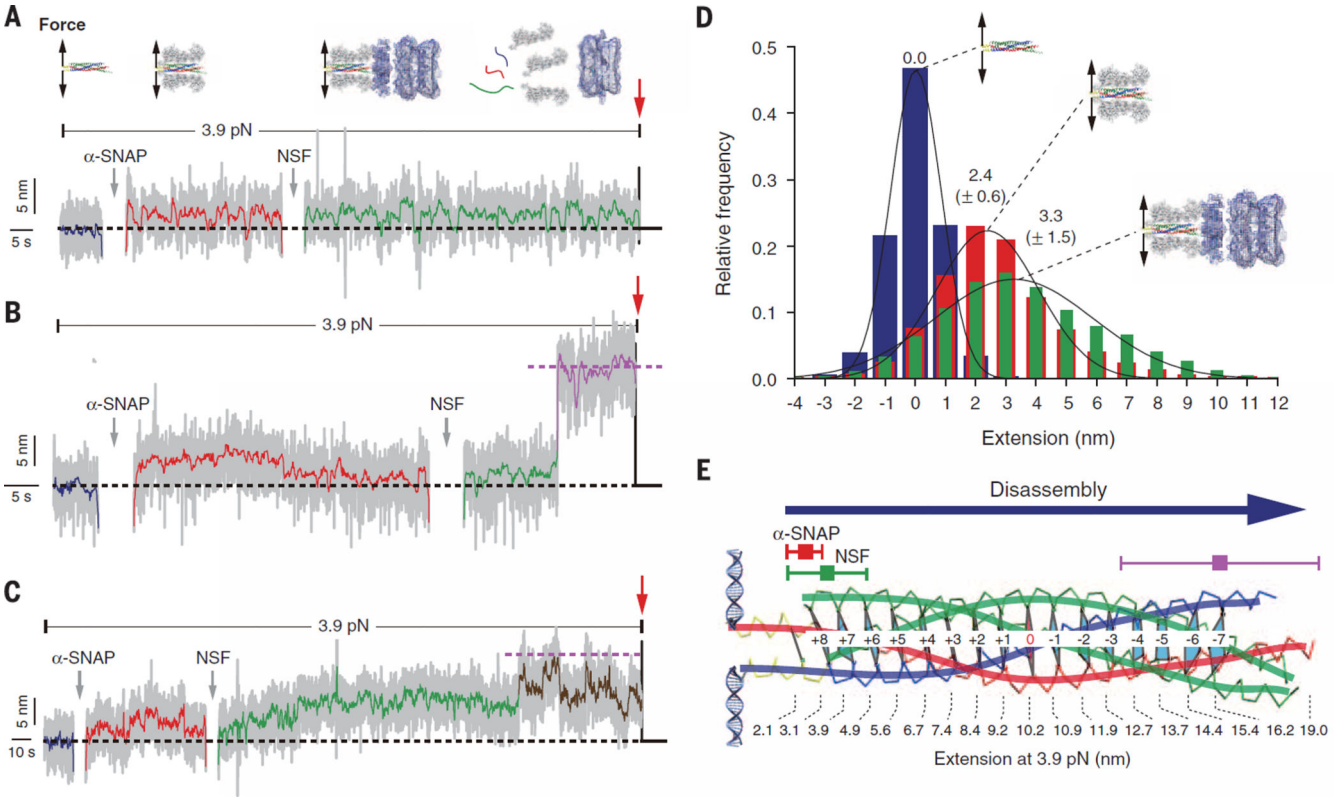

Fig. 3. Observation of NSF-mediated SNARE-complex disassembly with single-molecule magnetic tweezers

(**A** to **C**) Representative real-time traces showing destabilization and disassembly of SNARE complexes driven by α-SNAP and NSF. The traces are categorized according to the disassembly types: complete disassembly within a temporal resolution of 16.7 ms (A), almost complete disassembly but with a few seconds delay before the final release (B), and repetitive unzipping of almost full SNARE complex before the final release (C). Pink dotted lines in (B) and (C) denote the fully unzipped state up to the seventh layer. (**D**) Extension distributions of the sequential stages colored as blue, red, and green in the extension traces of (A) to (C) (*n* = 23 traces). (**E**) Structure diagram of the SNARE complex mapping the extension changes onto the corresponding positions in the structure. When a SNARE complex is unzipped to specific layers at 3.9 pN, the expected extension values are estimated with the wormlike chain model (shown at the bottom) (table S1). The positions of destabilizations (red for α-SNAP only and green for α-SNAP/NSF) and the position after the disassembly step (pink) are shown.

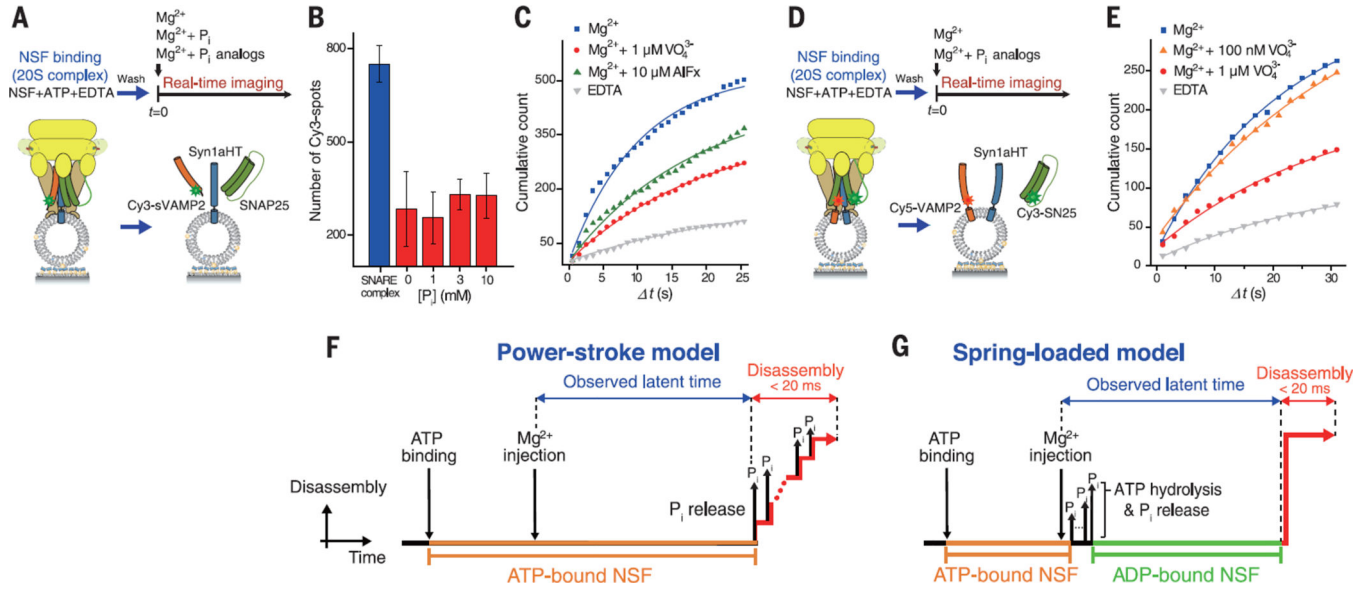

Fig. 4. Molecular model for disassembly of the SNARE complex mediated by NSF and α-SNAP

(**A**) Experimental design for sVAMP2 dissociation assay with Pi analogs. (**B**) Pi titration experiment. (**C**) Latency distributions of sVAMP2 dissociation via one-round ATP hydrolysis with Pi analogs. (**D**) Experimental design for SNAP-25 dissociation from the SNARE complex with full-length VAMP2 with Pi analogs. (**E**) Latency distributions of SNAP-25 dissociation with Pi analogs. (**F**) and (**G**) Mechanochemical model of the dwell-burst disassembly process for the power-stroke model (F) and the spring-loaded model (G).